Technical Sciences, 2017, 20(1), 31–48

UNIWERSYTET WARMIŃSKO-MAZURSKI W OLSZTYNIE

Quarterly peer-reviewed scientific journal
ISSN 1505-4675
e-ISSN 2083-4527
TECHNICAL SCIENCES
Homepage: www.uwm.edu.pl/techsci/

COMPARING SELECTED PARAMETERS OF A TWO-DIMENSIONAL TURBULENT FREE JET ON THE BASIS OF EXPERIMENTAL RESULTS, DIGITAL SIMULATIONS, AND THEORETICAL ANALYSES

Aldona Skotnicka-Siepsiak

Institute of Building Engineering
University of Warmia and Mazury

Received 27 September 2016, accepted 27 December 2016, available online 28 December 2016.

K e y w o r d s: 2D free jet, turbulent jet, CFD, spreading rate, velocity profiles, Coandă effect.

A b s t r a c t

The presented experimental and digital examinations of a two-dimensional turbulent free jet are a first phase of in the study of the Coandă effect and its hysteresis. Additionally, basing on theoretical analyses, selected results for a turbulent jest have been also mentioned, considering theoretical assumptions for the wall layer. As the result, on the basis of experimental, digital, and analytical methods, a review of characteristic jet properties has been prepared, which includes a jet spreading ratio, its cross and longitudinal sections, and turbulence level. The jet spreading radio has been expressed as a non-linear function of the $x : b$ relative length.

Introduction

The carried-out examinations aimed at identifying properties of a two-dimensional turbulent free jet basing on the results of obtained laboratory measurements, theoretical calculations, and CFD simulations carried out with the *FloVent* calculating application. They have been performed for the Reynolds number ranging from 10,000 to 38,000.

Correspondence: Aldona Skotnicka-Siepsiak, Instytut Budownictwa, Zakład Budownictwa Ogólnego i Fizyki Budowli, Uniwersytet Warmińsko-Mazurski, ul. Heweliusza 4, 10-724 Olsztyn, phone: 89 523 45 76, e-mail: aldona.skotnicka-siepsiak@uwm.edu.pl

As for the comparison of the obtained laboratory and theoretical results, we had a large set of previously conducted research analyses at our disposal. Our actions focused on confirming the convergence of our own results and previously carried-out examinations by other authors. The issue of estimating how the results of the digital simulations in *FloVent* may be applied was the next phase of our work; however, we did not have any previous results by other scientists here. In spite of the fact that the *FloVent* application was created mostly for assessing the issues of ventilation, it is mainly used for engineering purposes, in analyses of air distribution assessment, heat transfer, and heat comfort.

The scope of this article makes a first phase of the research works that assume an analysis of the Coandă effect hysteresis and its practical application at improving the air mix in systems based on the dilution principle (WIERCIŃSKI, GROMOW 2002).

The Coandă effect is named after Henri Marie Coandă whose research resulted in an American patent no. 2052869 "Device for Deflecting a Stream of Elastic Fluid Projected into an Elastic Fluid" in 1936 (Coanda 1936). The discovered phenomenon was applied widely: in 1938 in the USA (Coanda 1938), Henri Coandă patented a flying saucer, which he called "Aerodina Lenticulara". The constructor treated the mechanism as the one in which future applications of the discovered phenomenon would be the most important for aviation. Previously, the project has been an inspiration for constructors and scientists (HAQUE et al. 2015, MIRKOV, RASUO 2012a, b).

Presently, the Coandă effect has found its way to many technical solutions: from ordinary tools as electric toothbrushes to sports cars or frequent uses in aviation (WIERCIŃSKI, GROMOW 2002). The big application scale of that phenomenon is confirmed by the resources of the United States Patent and Trademark Office where the amount of 3,164 patent applications is displayed when searched for the patents applied after 1976 and referring to the keyword "Coandă".

However, until proposing final solutions is possible, we have focused on an initial case for us when a two-dimensional turbulent jet of diffused air is considered. Such a jet appears very often in practical ventilation issues. For instance, it is generated by slot diffusers. In the cases where a movement of the air flowing out of a diffuser takes place in an air medium that remains in relative stillness and is not limited by surfaces of the partitions forming a room, we can talk about a turbulent free jet (SZYMAŃSKI, WASILUK 1999). The Coandă effect may occur as a result of the closeness of a barrier, the angle that the jet flows, or the influence of another air jet (FAGHANI, ROGAK 2012). Adhesion of the air jet, e.g. to the surface of a ceiling, resulting from an inducted vortex and higher vacuum on one side when dimension a does not

exceed 50–30 thicknesses of the jet has been presented in the first case in Figure 1. A similar effect may be expected when angle h is less or equal to 45° (Fig. 1) (RECKNAGEL et al. 1994).

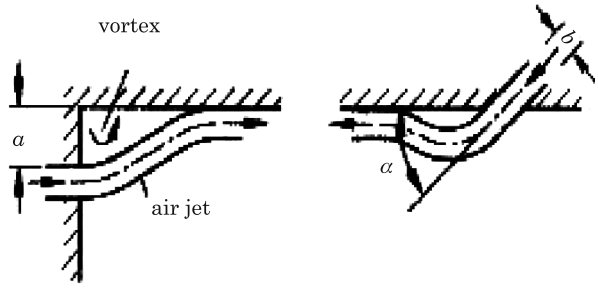

Fig. 1. The Coandă effect with air jets
Source: FAGHANI, ROGAK (2012).

By causing adhesion and sliding, the Coandă effect changes the designed air distribution in a room and it was usually perceived as an unfavourable phenomenon. Presently, the Coandă effect is used frequently in a planned way and is intended at the stage of conceptualization and implementation of air division in ventilated or air-conditioned rooms. Works by VON HOFF et al. (2012) or VALENTIN et al. (2013) may be provided here as an illustrations.

We hope that we are capable of using the potential of that phenomenon basing on the Coandă effect hysteresis in the construction of a diffuser. An unstable jet of air that alternatively adheres and comes unstuck of a barrier is to cause an improvement of the air mix and a decrease of speed and temperature gradients averaged in time for a room (WIERCIŃSKI, GROMOW 2002).

Literature Review

A turbulent isothermal jet of air was subjected to the analysis. The value of Re_{kr} = 1,200 was accepted as a limit of the laminar movement for plane slots.

Upon leaving the nozzle, the turbulent air jet starts to spread gradually which entails an increase of its cross section and a decrease of velocity. Moreover, a movement of air particles in the transverse direction towards the direction of the jet is observed in the turbulent jet, which effects in transporting the particles outside the main mass of the jet. The particles transport kinetic energy to the bordering layers of the surrounding air and grab some particles from the surrounding air towards the jet.

Four zones of the following properties may be distinguished in the air jet:

Zone I: initial – characterized by the unchangeability of its axial velocity. In it, a jet core can be separated where the initial velocity is sustained. The smaller the vortices of the jet are, the longer zone is.

Zone II: transitory – a distribution of velocities characteristic for turbulent free jets is shaped in its cross-section profile. Its length depends on the construction of a diffuser.

Zone III: basic – there is a proportional decrease of its axial velocity in relation to the length from the outlet

Zone IV: dominant influence of viscous forces – together with a rapid decrease of its axial velocity, the jet stops along its primary axis.

In the case of a plane jet, a decrease of its axial velocity is much smaller than in the case of a round one, which results its farther reach.

According to the information in the article by NEWMAN (1961), the static pressure in the jet is the same everywhere, thus the jet momentum is constant regardless of a distance from the nozzle. A flow in defined length x along the jet, for a jet from the slot with width b and core velocity U, may be as well formed by a bigger slot with width b' and a lower value of velocity in the jet core U', located somewhere along the flow of the jet.

$$\rho\, U'^2\, b' = J = \rho\, U^2\, b \tag{1}$$

where:

ρ – density,
U, U' – velocity at the nozzle outlet,
b, b' – width of the diffusion slot,
J – value of jet momentum in relation to the width unit of the nozzle.

The value of mean velocity u in distance y from the middle of the jet depends on jet momentum J, fluid density ρ, and the x, y localization in the accepted frame of reference. When moving further from the stable area, e.g. with participation of free turbulences, it may be assumed that the change in the fluid viscosity is of no significant influence on the flow or on the large-scale vortices.

The value of localization $y_{m:2}$, for which the mean velocity measured perpendicularly to the jet axis reaches the $u = {}^1/_2\, u_m$, value of a half of the maximal velocity in a given cross-section of profile velocity may be accepted as a measure of the jet spreading in a local frame of reference towards direction y, measured perpendicularly to the jet axis.

For all the x values in the accepted frame of reference, the following similarity for the profiles of velocity diffusion is accepted:

$$\frac{u}{u_m} = F\left(\frac{y}{y_{m:2}}\right) \tag{2}$$

According to the Görtler's assumptions, it can be accepted that turbulent viscosity *4* is constant across the flow for every x value and proportional to the $u_m\ y_{m:2}$ value. The solution is formed as follows:

$$u = u_m \sec h^2 \frac{0.88y}{y_{m:2}} = \left\{\frac{3\ J\sigma}{4\ \rho x}\right\}^{\frac{1}{2}} \sec h^2 \frac{\sigma y}{x} \tag{3}$$

where:
σ – constant,
u_m – maximal velocity value in a given section.

The above dependence occurs for the conditions when y <1.3 $y_{m:2}$; in other cases it provides slightly too high results. The flow is not independent from slot width b until the $x : b$ value reaches 25. The results by Bourque provide the value of $\sigma = 12$ close to the nozzle that falls down to the value of 7.5 for large $x : b$ values. When accepting the value of $\sigma = 7.7$, we obtain:

$$y_{m:2} : x = 0.88 : \sigma = 0.114$$

$$\rho\ u_m{}^2\ x : j = 3\sigma : 4 = 5.78 \tag{4}$$

$$\varepsilon : u_m\ y_{m:2} = 1 : 3.52\ \rho = 0.037$$

where:
ε – turbulent viscosity.

Localization of value $y_{m:2}$, for which the velocity measured perpendicularly to the jet axis reaches the $u = {}^1/_2\ u_m$ value of a half of the maximal velocity in a given cross-section velocity profile complies also to:

$$\frac{y_{m:2}}{b} = K_1\left(\frac{x}{b} + K_2\right) \tag{5}$$

where:
K_1, K_2 – coefficient.

Coefficient K_1 is a measure of the jet spreading ratio, and using the following dependency:

$$x_0 = -K_2 b \tag{6}$$

it is possible to identify a localization of a virtual origin of jet x_0 (KOTOSOVINOS 1976). Information on localization of the virtual origin is equivocal. Some part of the researchers place it in front of the nozzle, others – behind it.

Attention should also be paid that directly behind the nozzle there is an area of the jet core, the length of which is approximately $6b$, which in the case of our calculations – for a diffusion slot with the width of $b = 20$ mm – means that the reach of the core area is up to the length of about $x_0 = 0.12$ m (RAJARATNAM 1976). In that area the dependencies indicated above will not to occur.

Description of Measuring Post

The laboratory measurements were taken at a measuring post in the laboratory of the Department of Building Engineering and Building Physics at the University of Warmia and Mazury in Olsztyn. The experimental results were performed as a part of the doctoral thesis, whose topic was "Hysteresis of the Coanda effect". Prof. Zygmunt Wierciński was the supervisor of the doctoral dissertation in the Institute of Fluid-Flow Machinery Polish Academy of Sciences. The examinations were performed in a chamber with dimensions of $385 \times 200 \times 229$ cm where a case made of transparent Plexiglas slates was fixed on a steel rack, which eliminated influences of the external environment on the conducted experiment. The air was delivered to the system by a sucking duct, 250 mm in diameter and 530 cm in length, placed 40 cm above the floor. On its inlet, the duct was equipped with an air intake, 400 mm in diameter, with a regulated flow. The duct was also equipped with a measuring orifice plate with impulse orifices in lengths D and $D/2$ to measure the static pressure. The orifices were connected to a pressure transducer by elastic hoses. A diffuser in the shape of the Witoszyński nozzle with regulated cross-section was mounted on the pressing side of the ventilator. The stable height of the nozzle was $h = 60$ cm. The experiments were performed for the nozzle width of $b = 2.0$ cm.

The experimental examinations were carried out for six measuring sessions characterized by various values of airflow for the Reynolds number ranging from about 10,000 to about 38,000. The symmetry centre in the frontal plane of the diffusion orifice of the Witoszyński nozzle forms the beginning of the frame. The accepted theoretical axis of the x jet is convergent with the axis of symmetry of the aforementioned nozzle, the width of which was 0.02 mm. All

the measurements were performed in plane $z = 0$ in the middle of the nozzle that was 0.60 m tall.

The scheme of the described measuring post has been presented in the Figure 2 below.

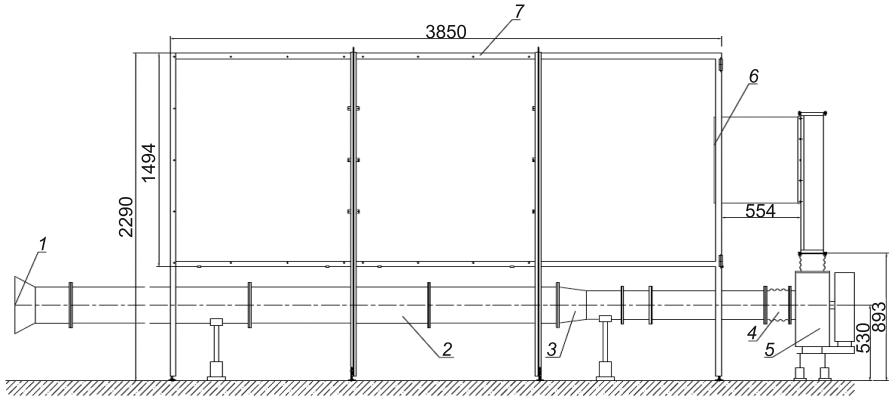

Fig. 2. Scheme of measuring post – side view: *1* – air intake with the flow regulated by a rotating element, *2* – sucking duct, *3* – orifice plate for measuring static pressure, *4* – ventilator, *5* – elastic joints, *6* – the Witoszyński nozzle, *7*- measuring post case made of a rack and Plexiglas slates

Distributions of the arithmetical mean for the velocity and the turbulence level of a turbulent free jet were examined using a thermo-anemometer ATU 2001.

In the above measuring system, we applied a dynamic measuring net that, while assuming optimization of the measuring points, was adjusted to the varied distribution of velocities in the examined air jet. The measurements were taken in 11 measuring lines parallel to each other. Vertically, they were localized in the axis of symmetry of the air diffusion. The first measuring line was directly behind the nozzle in the minimal length of $x : b = 0.5$, which was allowed for by the construction of the stand of the thermo-anemometric probe. The measurement was taken in the jet core. The following measuring lines were situated every 0.10 m away from the nozzle towards direction *x,* until the final value of $x : b = 50.0$ was reached Every measuring line was characterized by is specific width resulting from the velocities identified at the measuring post. The measurements for every measuring line were carried out in a local frame of reference toward direction ±y, until the velocity values lover than 1 m/s were recorded.

Table 1 contains a list of values for the ventilator capacities, the velocities at the outlet from the nozzle identified on the basis of measurements taken with the orifice plate and the hot wire, as well as the value of the Reynolds number for every measuring session.

Table 1

Values of ventilator capacities, air velocities at the nozzle outlet and the Reynolds

Measuring session	Ventilator capacity	Air velocity at nozzle outlet		Reynolds number
		based on measurements with orifice place	based on measurements with thermoanemometer	
	[m^3/s]	[m/s]		[–]
1	0.338	28.19	28.02	37,343
2	0.250	20.90	20.78	27,685
3	0.152	12.67	12.86	16,784
4	0.127	10.56	10.18	13,983
5	0.107	8.88	8.63	11,768
6	0.096	7.98	7.98	10,570

The values of the Reynolds number were calculated according to the formula:

$$\mathrm{Re} = \frac{U \cdot b}{v} \tag{7}$$

where:
U – velocity at the nozzle outlet,
b – width of the diffusion slot,
v – coefficient of kinematic viscosity.

Due to the fact that the measuring post was situated in a confined space of the laboratory room, from which the circulatory air for the measuring system was collected, it was accepted for simplicity reasons that the measuring system is an isothermal one.

Measuring Net for the Turbulent Free Jet

Using the Computational Fluid Dynamics (CFD), a digital model of the aforementioned laboratory post was created and simulations were conducted, which made it possible to examine distributions of the arithmetic mean for the velocity and turbulences of a turbulent free jet. The simulations were carried out using the *FloVent* application by *Mentor Graphics*.

The examinations were conducted for each of the six measuring sessions, for the air capacity in the system identified experimentally and for the diffusion slot $b = 20$ mm wide.

A measuring net consisting of about 500,000 meshes was used in the simulation. In the area where the parameters of the turbulent free jet were analysed the net was concentrated and the dimensions of a mesh were $x = 5$ mm, $y = 20$ mm, $z = 30$ mm (the directions according to the *FloVent* scheme). The dimensions of the area were $x = 1.20$ m, $y = 0.62$ m, $z = 1.00$ m. As for the remaining area of the measuring post, the meshes did not exceed 75 mm in every direction.

The application provides three models of turbulence: *Capped LVEL*, *LVEL Algebraic,* and *LVEL K-Epsilon*. The *LVEL K-Epsilon* model was used for the simulations as it is the one that had been verified in the largest number of engineering calculations and, according to the producer's information, it provided the best results. The model is also characterized by simplicity and stability.

The calculations were performed by a computer equipped with a CPU 2.61 GHz and 3.25 GB of RAM. The running time for a single simulation was about 2.5 hours.

Calculation Results

The calculations of the jet momentum carried out according to formula (1) provided the results: Re = 37,343 → 18.60 kg/s^2; Re = 27,685 → 10.42 kg/s^2; Re = 16,784 → 3.73 kg/s^2; Re = 13,983 → 2.61 kg/s^2; Re = 13,983 → 1.86 kg/s^2 and Re = 10,570 → 1.49 kg/s^2. The jet momentum is a constant value, regardless of the length from the nozzle.

In order to analyse the distribution of velocities in the jet, for the diffusion slot with the width of $b = 20$ mm, the u_m value of the maximal velocity was verified in particular measuring planes basing on the experimental data. Generally, the assumption that maximal values in particular measuring planes were within jet axis $x : b = 0.0$ was confirmed. The distribution of velocity was identified using formula (3). Values of the σ parameter shown in Table 2, were accepted for calculations. In our case, the mean value of the σ coefficient out of the area of the jet core ($x : b = 10.0 \div 50.0$) was 8.10. It is a higher value than the ones given in the literature (NEWMAN 1961). A higher accordance occurred for sessions 4, 5, and 6 that were characterized by lower values of Re = 10,000 ÷ 15,000.

The analysis of theoretical calculations and the CFD simulation of the u_m values of the maximum velocity in particular measuring planes, which were

obtained on the basis of laboratory measurements, indicates that the average difference in the obtained values of u_m for particular measuring plates is 1.9% for comparable research methods. When comparing the results obtained by theoretical calculations and laboratory measurements, the maximal differences in the u_m value of the maximum velocity did not exceed 0.7%, and the average difference was 0.2%. A comparison of the data obtained by measurements and CFD simulations provides worse results. In spite of a satisfactory mean value of deviations on the level of 3.6%, some quite huge deviations of up to 10.6% may be observed in particular profiles.

Table 2

Values of the σ parameter accepted in calculations; width of the diffusion slot b = 20 mm

$x : b$ [–]	Values of the σ parameter [–] for measuring session:					
	1 Re = 37,343	2 Re = 27,685	3 Re = 16,784	4 Re = 13,983	5 Re = 11,768	6 Re = 10,570
0.5	0.66	0.67	0.69	0.62	0.63	0.66
5.0	6.40	6.60	6.00	5.20	5.60	5.40
10.0 ÷ 50.0	8.47	8.30	8.78	8.07	7.38	7.58

The analysis of the relation between the u_m value of the axial velocity in particular measuring planes and the U value at the outlet of the nozzle for selected measuring sessions is presented in Figure 3.

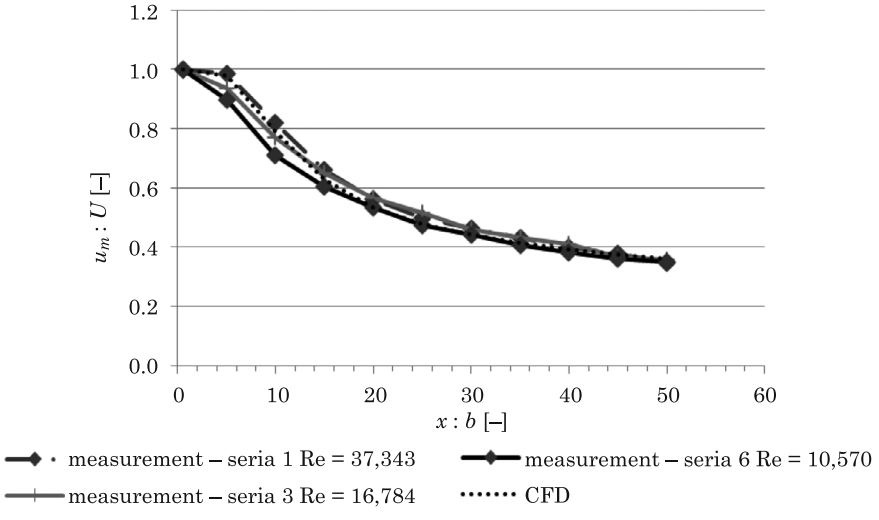

Fig. 3. Correlation between the u_m value of the axial velocity in measuring planes and the U value at the outlet of the nozzle for selected measuring sessions 1, 3 and 6

The course of the curve mirroring the results of the CFD simulation is unchangeable for all the measuring sessions. A very high convergence of the results obtained by laboratory measurements and theoretical calculations makes it possible to accept the convergence of the curves mirroring the results. However, they are different for particular measuring sessions. For measuring sessions with the higher values of the Reynolds number, it is visible that the results obtained by the CFD simulations are understated in the middle part of the jet. As the Reynolds number decreases, an increase in the CFD simulation results is visible for the first three measuring planes. As for the further measuring planes, understating of the obtained results of simulations is visible, as well as accordance of the results for the last two measuring sessions. In the case of the lowest values of the Reynolds number, the convergence occurs in the middle part of the jet; however, in the remaining areas, the simulation results are overstated in relation to the laboratory results and the ones obtained from theoretical calculations.

An examination of the decrease in the u_m value of axial velocity in particular measuring planes may be also conducted on the basis of the following formula:

$$\frac{u_m}{U} = \sqrt{\frac{b}{m \cdot x}} \tag{8}$$

where:
m – mixed number.

The value of mixed number obtained in such a way is $m = 2.00$ for the first measuring plane localized directly behind the nozzle at $x = 0.01$ m in the area of the jet core, regardless of the manner of identification of the u_m axial velocity in particular measuring planes. In the next measuring plane, for $x = 0.10$ m, there occurs a significant decrease in the value of the m coefficient. As for the results of the CFD simulations, the value $m = 0.21$ was obtained, regardless of the Reynolds number. In the case of the mixed coefficient determined on the basis of laboratory examinations and theoretical calculations the following dependency is visible: as the value of the Reynolds number increases, the value of the m coefficient decreases. In the following planes, in spite of small fluctuations, the value of the m coefficient is equalized. As for the results obtained by the CFD simulations, it is $m = 0.16$ for all the measuring sessions. In the case of the remaining examination methods, the previously observed dependency between the values of the Reynolds number and the m coefficient is observed. The values of mixed number m for three selected measuring sessions are shown in Table 3.

The analysis of the turbulence level based on laboratory examination confirms the fact that the measurement in the first measuring plane for $x : b = 0.5$ is situated in the diffused air jet core. The measurements taken in the following planes indicate that the jet is shaped gradually, while the measurement in the second plane for $x : b = 5.0$ points out at the localization in the transitory zone of the jet. The jet spread increases together with the increase of the length from the diffuser, with the simultaneous decrease of the turbulence level. However, lacks of total similarity and fully shaped turbulence profiles are visible, which is to be obtained for our diffusion slot with the width of $b = 20$ mm on exceeding the length of $x : b > 65.0$ from the nozzle according to the rule defined by RAJARATNAM (1976). The described dependencies are presented in Figure 4.

Table 3

Values of mixed number m

$x : b$ [–]	Value of mixed number m [–] for measuring session:								
	1 Re = 37,343			3 Re = 16,784			6 Re = 10,570		
	Measurement	Theoretical Calculation	CFD Simulation	Measurement	Theoretical Calculation	CFD Simulation	Measurement	Measurement	Measurement
0.5	2.00	2.00	2.00	2.00	2.00	2.00	2.00	2.00	2.00
5.0	0.21	0.21	0.21	0.23	0.23	0.21	0.25	0.25	0.25
10.0 ÷ 50.0	0.16	0.16	0.16	0.16	0.16	0.16	0.18	0.18	0.18

When examining spreading of the jet, in a local frame of reference towards the y direction measured perpendicularly to the jet axis, localization $y_{m:2}$ was considered, for which the mean velocity measured perpendicularly to the jet axis reaches the $u = {}^1/_2\, u_m$ value for a half of the maximum velocity in a given cross-section profile of velocity. The values may be accepted as convergent ones, apart from the areas of the jet core and the transitory zone (the first two measuring planes) that were omitted in the further analysis. In the case of comparing the $y_{m:2}$ localization identified on the basis of the measurement data and theoretical calculations, the average difference in the obtained coordinates is ±7 mm ($y : b = 0.35$). It is noteworthy that the worst matches in the studied scope occur in measuring sessions 5 and 6 (the average difference in the obtained coordinates is ±12 mm –$y : b = \pm 0.6$). The convergence of the results obtained from the laboratory measurement and the CFD simulations appears to be slightly worse. The average difference in the obtained localization coordinates towards direction y is ±8 mm ($y : b = \pm 0.4$). Regardless of the applied calculation methods, the maximum difference in the obtained localiz-

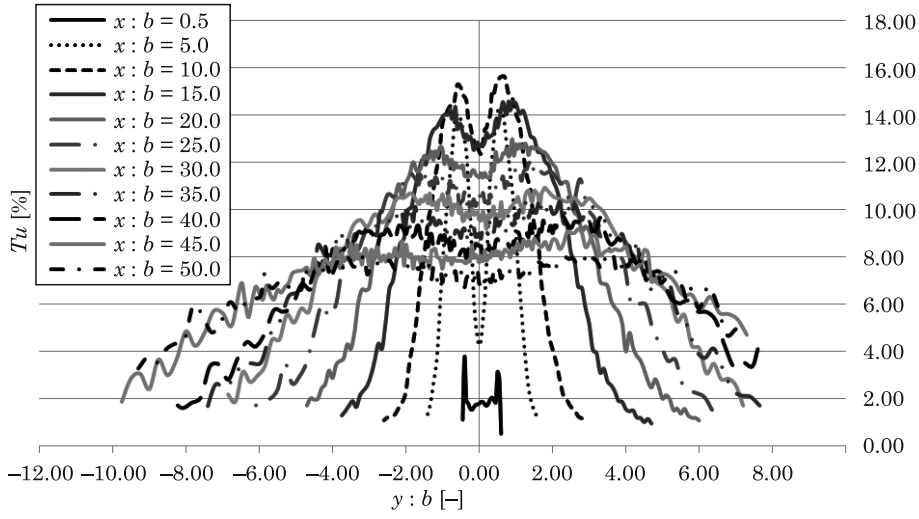

Fig. 4. Turbulence level Tu based on the laboratory examinations for a diffusion slot with the width of b = 20 mm; measuring session no 1 Re = 37,343

ation coordinates towards direction y does go beyond ±3.5 cm ($y : b = \pm 1.75$). A very high convergence of the $y_{m:2}$ localization is visible for the results obtained by the CFD simulation. It is virtually the same for all the measuring sessions regardless of the noted various $u = {}^1/_2\, u_m$ values for velocity.

The described dependencies are illustrated by the sample Figure 5.

In spite of the convergence of the identified u_m maximum velocity in the measuring plane situated directly behind the diffuser at $x : b = 0.5$, the shape of the curve illustrating the distribution of the velocity is divergent when laboratory, theoretical, and CFD simulation results are compared. This entails the fact that the localization of the $u = {}^1/_2\, u_m$ value for a half of the maximum velocity is also divergent. It is a result of the fact that the first measuring plane was localized in the area of the jet core, where it still was not shaped and was not convergent with the theoretical description of the jet shape. In the measuring planes at lengths of $x : b > 5.0$, the image of the already-shaped jet is in accordance with the theoretical assumptions (Fig. 5); however there is a divergence visible here for the u_m values of the maximum velocity determined by the CFD simulations and the remaining methods. In the case presented on the graph, it is about 5.5%.

Basing on the identified localization of the $u = {}^1/_2\, u_m$ value for a half of the maximum velocity, the jet spreading angle was analysed by applying three methods of examining velocity distribution (Tab. 4).

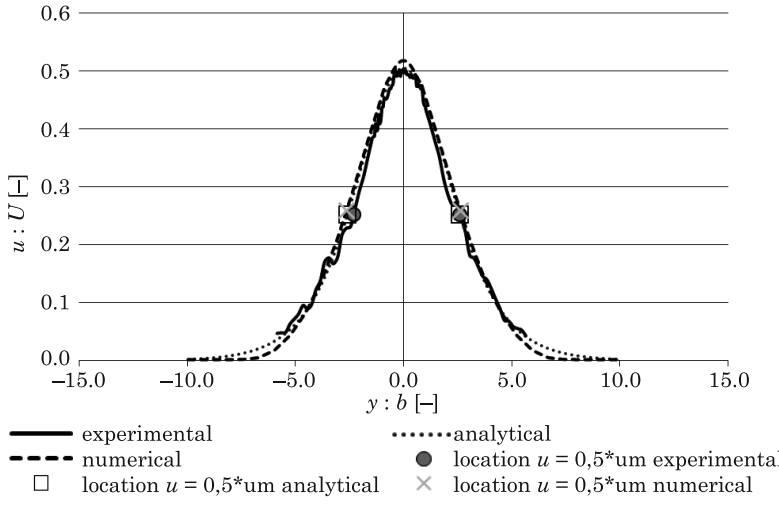

Fig. 5. Velocity values for the slot width of b = 20 mm; the measuring plane at the length of $x : b$ = 25.0; measuring session 2: Re = 27,685

Table 4

Jet expansion angle α [°]

Specification	Jet expansion angle α [°] for measuring sessions 1–6					
	1 Re = 37,343	2 Re = 27,685	3 Re = 16,784	4 Re = 13,983	5 Re = 11,768	6 Re = 10,570
Laboratory measurement	12.05	13.72	15.55	15.49	14.24	13.84
Theoretical calculation	12.55	13.82	11.47	11.49	14.42	12.15
CFD simulation	13.14	13.14	13.13	13.13	13.13	13.13

For the measuring sessions no 1, 2 and 5, the values of the jet spreading angle determined from the results of the theoretical calculations are convergent with the laboratory results. In the remaining cases, some huge divergences, up to 4°, are visible. A general trend for a decrease of the spreading angle together with an increase of the Reynolds number is visible in the laboratory results. As for the results obtained in the CFD simulations, the value of spreading angle α = 13.1° is obtained for all the measuring sessions.

The analysis of the virtual jet origin localization requires considering the values of coefficients K_1 and K_2 according to formulas (5) and (6) presented before. As the results of theoretical calculations and simulations are not comparable with the laboratory results for the first two measuring planes, those planes were omitted in the further analysis.

In the case of the laboratory measurements that we carried out, provided that the first two measuring planes were omitted in the analysis, the virtual jet origin was always localized behind the diffuser ($K_2 < 0$). The analysis of the results obtained by theoretical calculations for the first three measuring sessions indicates that the localization of the virtual jet origin is behind the nozzle; however, the remaining three cases indicate that its localization is in front of it. As for the results obtained from the CFD simulations, the virtual jet origin is located in front of the nozzle, practically in the same point each time for all the measuring sessions. Figure 6 presents those dependencies.

It is noteworthy that the results obtained by theoretical calculations correspond in the best way with the linear dependency trend of coefficients K_1 and K_2 identified on the basis of the literature data (KOTSOVINOS 1976). The values of the K_1 jet spreading coefficient that we obtained by analysing the laboratory measurements are higher than the data from the literature (KOTSOVINOS 1976).

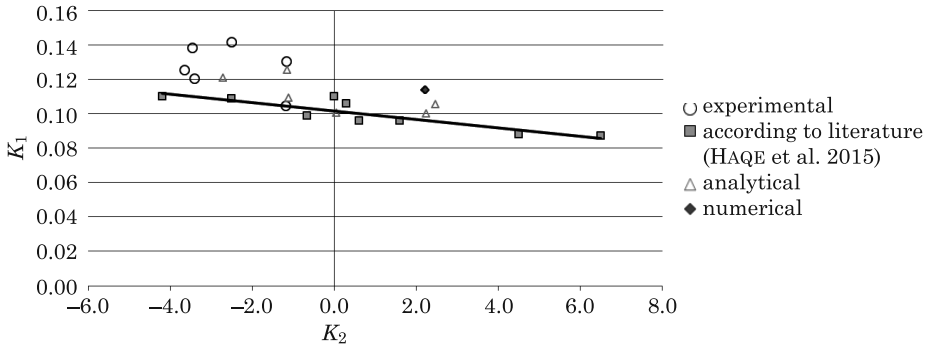

Fig. 6. Dependency between coefficients K_1 and K_2

In own research, $K_1 = 0.105 \div 0.142$ and $K_2 = -3.65 \div -1.17$ for laboratory examination. In case of theoretical calculations the coefficient $K_1 = 0.100 \div 0.126$ and $K_2 = -2.71 \div 2.47$. For numerical investigations the $K_1 = 0.114$ while $K_2 = 2.22 \div 2.23$. Those results have a good compatibility with the literature (KOTSOVINOS 1976) referring

The obtained results of the σ parameter analysed in the context of the dependency: $y_{m:2} : x = 0.88 : \sigma = 0.114$ cited in formula (5) after (NEWMAN 1961) show a convergence for the area of a formed turbulent jet. In the case of measuring sessions with the lowest values of the Reynolds number, the probability of the obtained results is the highest.

Table 5

Analysis of distribution of the 0.88 : σ value for particular measuring sessions

$x : b$ [–]	Values of 0.88 : σ [–] for measuring session:					
	1 Re = 37,343	2 Re = 27,685	3 Re = 16,784	4 Re = 13,983	5 Re = 11,768	6 Re = 10,570
0.5	1.333	1.313	1.275	1.419	1.397	1.333
5.0	0.138	0.133	0.147	0.169	0.157	0.163
10.0 ÷ 50.0	0.104	0.106	0.100	0.109	0.119	0.116

The thesis that the distribution of an increased value of the localization for which the mean velocity measured perpendicularly to the jet axis reaches the $u = {}^1/_2 u_m$ value for a half of the maximum velocity in a given velocity cross-section profile for the analysed turbulent jets is not precisely linear, cited after (KOTSOVINOS 1976), was also confirmed.

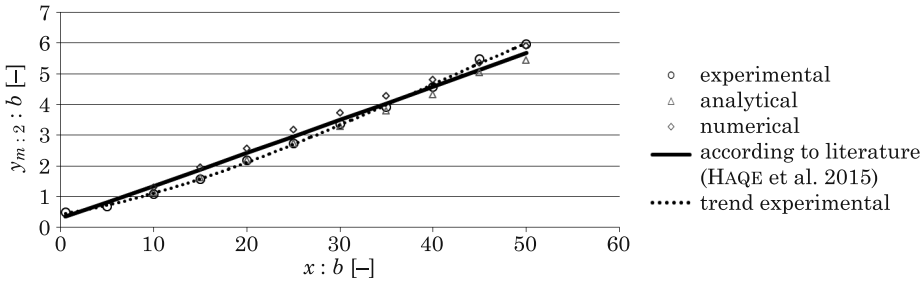

Fig. 7. Distribution of the $y_{m:2}$ localizations to b along the jet for the mean results of all the measuring sessions

Following (KOTSOVINOS 1976), presented in Figure 7 is a curve of the following formula:

$$\frac{y_{m:2}}{b} = 0.228 + 0.0913\,\frac{x}{b} + 0.00005101\left(\frac{x}{b}\right)^2 + 0.000000331\left(\frac{x}{b}\right)^3 \qquad (9)$$

according to which the characteristics of the distribution was presented by the author. The trend line charted for the mean results of own laboratory results is described by the formula:

$$\frac{y_{m:2}}{b} = 0.4317 + 0.0489\,\frac{x}{b} + 0.0021\left(\frac{x}{b}\right)^2 + 0.00002\left(\frac{x}{b}\right)^3 \qquad (10)$$

It diverges from the curve defined in the literature; however, attention should be paid at the fact that the analyses that we have conducted apply only to the area of $x \leq 50\ b$, while in the literature (KOTSOVINOS 1976) the area it four times longer.

Conclusions

The obtained results confirm a possibility to examine the properties of a two-dimensional turbulent free jet on the basis of the obtained laboratory measurements, theoretical calculations and CFD simulations carried out by the *FloVent* calculating application.

The conducted examinations did not made it possible for us to find a satisfactory answer to the question of virtual jet origin localization. The results based on digital examinations indicate that it is localized in front of the diffusion nozzle. However, the results based on the laboratory measurements and theoretical calculations do not provide an unequivocal answer indicating localizations both behind and in front of the nozzle. The obtained values of the K_1 coefficient are the most convergent with the results by Flora & Goldschmidt, Heskestad, Kotsovinos, Mih & Hoopes, or Nakaguchi cited from the literature (KOTSOVINOS 1976).

References

BOURQUE C., NEWMAN B.G. 1959. *Reattachment of a Two-Dimensional Incompressible Jet to an Adjacent Plane Plate*. Aeronaut. Quarterly, 11: 201.

COANDA H. 1936. *Device for deflecting a stream of elastic fluid projected into an elastic fluid*. United States Patent 2052869. http://www.freepatentsonline.com/2052869.html (access: 09.12.2016).

COANDA H. 1938. *Propelling device*. United States Patent 2108652. http://www.freepatentsonline.com/2108652.html (acess: 09.12.2016).

FAGHANI E., ROGAK S.N. 2012. *Application of CFD and Phenomenological Models in Studying Interaction of Two Turbulent Plane Jets*. International Journal of Mechanical Engineering and Mechatronics, 1(1).

FÖRTHMANN E. 1934. *Über turbulente Strahlausbreitung*. Ing.-Archiv, 5(42).

GÖRTLER H. 1942. *Berechnung von Aufgaben der freien Turbulenz auf Grund eines neuen Naeherungsatzes*. ZAMM, 22: 244.

HAQUE E., HOSSAIN S., ASSAD-UZ-ZAMAN M., MASHUD M. 2015. *Design and construction of an unmanned aerial vehicle based on Coanda effect*. Proceedings of the International Conference on Mechanical Engineering and Renewable Energy (ICMERE2015), 26–29 November, Chittagong, Bangladesh.

HOOFF T. VAN, BLOCKEN B., DEFRAEYE T., CARMELIET J., VAN HEIJST G.J.F. 2012. *PIV measurements and analysis of transitional flow in a reduced-scale model: Ventilation by a free plane jet with Coanda effect*. Building and Environment, 56: 301–313.

KOTSOVINOS N.E. 1976. *A Note on the Spreading Rate and Virtual Origin of a Plane Jet*. The Journal of Fluid Mechanics, 77(2): 305–311.

MIRKOV N., RASUO B. 2012. *Manoeuvrability of an UAV with Coanda effect based lift production*. 28th International Congress of the Aeronautical Sciences.

MIRKOV N., RASUO B. 2012. *Numerical simulation of air jet attachment to convex walls and applications*. 28th International Congress of the Aeronautical Sciences.

NEWMAN B.G. 1961. *The Deflexion of Plane Jet by Adjacent Boundaries – Coandă* Effect. Pergamon Press, Oxford.

RAJARATNAM N. 1976. *Turbulent Jets*. Elsevier Scientific Publishing Company, Amsterdam – Oxford – New York.

RECKNAGEL H., SPRINGER E., HÖNMANN W., SCHRAMEK E.R. 1994. *Poradnik ogrzewanie i klimatyzacja*. EWFE, Gdańsk.

REICHARDT H. 1943. *On a New Theory of Free Turbulence*. J. Roy. Aero. Soc., 47: 167.

SZYMAŃSKI T., WASILUK W. 1999. *Wentylacja użytkowa poradnik*. IPPU Masta, Gdańsk.

VALENTÍN D., GUARDO A., EGUSQUIZA E., VALERO C., ALAVEDRA P. *Use of Coand)a nozzles for double glazed fac(ades forced ventilation*. Energy and Buildings, 62: 605–614.

WIERCIŃSKI Z., GROMOW E. 2002. *Polepszenie rozdziału powietrza w pomieszczeniu wentylowanym za pomocą niestacjonarnego efektu Coandă*. Ciepłownictwo Ogrzewnictwo Wentylacja, 10.